IMAGE: A MAP OF THE STARS OF THE ORION CONSTELLATION

Print ISSN: 2631-8474 Online ISSN: 2631-8482

JournalPreview

London Journal of Engineering Research

Volume 21 | Issue 3 | Compilation 1.0

London Journals Press

WWW.JOURNALSPRESS.COM

JournalPreview

LONDON JOURNAL ENGINEERING RESEARCH

Journal Content
In this Issue

London Journals Press

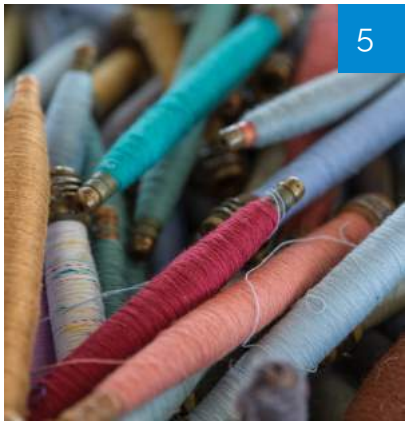

About Generating Electricity by a Solar Module at Night

Aleksandr Ivanovich Kanareykin

University Sergo Ordzhonikidze

ABSTRACT

The work is devoted to the issue of generating electric energy by a solar module at night. The article presents the conclusion of the formula for calculating the no-load voltage of the module. The obtained result makes it easier to find this parameter because the desired value is determined mainly by the technical parameters of the solar module.

Keywords: solar energy, solar battery, night time, idle mode, maximum powerpoint.

Classification: FOR Code: 090699

Language: English

London Journals Press

LJP Copyright ID: 392981
Print ISSN: 2631-8474
Online ISSN: 2631-8482

London Journal of Engineering Research

Volume 21 | Issue 3 | Compilation 1.0

About Generating Electricity by a Solar Module at Night

Aleksandr Ivanovich Kanareykin

ABSTRACT

The work is devoted to the issue of generating electric energy by a solar module at night. The article presents the conclusion of the formula for calculating the no-load voltage of the module. The obtained result makes it easier to find this parameter because the desired value is determined mainly by the technical parameters of the solar module.

Keywords: solar energy, solar battery, night time, idle mode, maximum powerpoint.

Author: Russian State Geological Exploration University named after Sergo Ordzhonikidze, Miklouho-Maclay St., 23, Moscow, 117997, Russia.

I. INTRODUCTION

As you know, the Sun is the source of life on the planet Earth. Today, one of the promising areas of energy supply to consumers is the development and introduction of renewable energy sources [1, 2].

There are also many works in the literature devoted to optimizing and increasing the efficiency of solar panels [3-7] since renewable energy sources are gaining more and more popularity all over the world every year. The most dynamically developing direction in this field is photovoltaics, the practical significance of which is the direct conversion of solar radiation energy into electricity.

A solar battery is a semiconductor device that converts sunlight into electrical energy. It is a p-n junction with ohmic contacts (fig. 1).

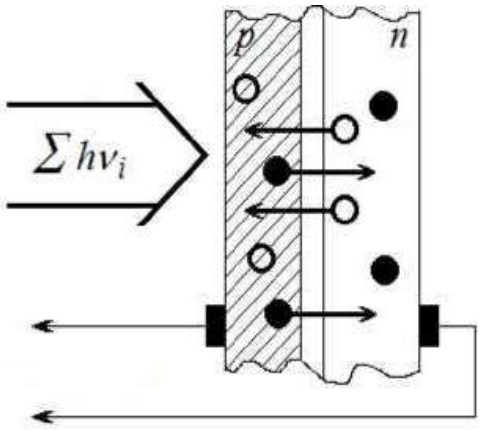

Figure 1: The structure of the solar battery

Solar radiation is converted into electrical energy of constant current by solar cells. Most solar cells are silicon semiconductor photodiodes. The energy characteristics of solar cells depend on the following parameters: the intensity of solar radiation, the magnitude of the load, the operating temperature.

If the energy of the light quanta is greater than the bandgap of the p-n junction semiconductors, then electron-hole pairs are generated under the action of light. They are separated by a potential barrier field in the transition region and move to the n-and p-regions, the basic carriers. As a result, electrons in the n-region and holes in the p-region become in excess, and these regions acquire negative and positive charges, respectively. In the absence of a load, the accumulation of charges causes a decrease, and even the disappearance of a potential barrier. As a result, the separation of pairs stops. There comes a state of equilibrium-saturation. The voltage that occurs in such a state at the p-i-junction is called the opening or idling voltage U_{xx}. By connecting an external circuit to the device, you can take away electricity. At night, the panel receives light from the stars and the moon.

In this regard, the question arises about the generation of electricity by solar panels at night.

II. MATERIALS AND METHODS

The paper uses the method of approximate calculation.

III. RESULTS

In the idle mode, the voltage of the solar module is equal toIn the idle mode, the voltage of the solar module is equal to

$$U_{oc} = \frac{kT}{Aq} \ln\left(\frac{J_s}{J_{os}} + 1\right) \quad (1)$$

where: k is the Boltzmann constant ($k = 1.38 \cdot 10^{-23}$ J/K), e is the elemental charge ($q = 1.6 \cdot 10^{-19}$ C), A is the coefficient, J_{os} is the saturation current, J_s is the reverse photocurrent.

With $J_s >> J_{os}$, the expression (1) will take the form

$$U_{oc} = \frac{kT}{Aq} \ln\left(\frac{J_s}{J_{os}}\right) \quad (2)$$

Let's find the ratio of the no-load voltages during the day U_{ocd} and at night U_{ocn}

$$\frac{U_{ocd}}{U_{ocn}} = \frac{\ln\left(\frac{J_{sd}}{J_{os}}\right)}{\ln\left(\frac{J_{sn}}{J_{os}}\right)} = \log_{\left(\frac{J_{sn}}{J_{os}}\right)}\left(\frac{J_{sd}}{J_{os}}\right) \quad (3)$$

If we express one expression as a power of another

$$\frac{J_{sd}}{J_{os}} = \left(\frac{J_{sn}}{J_{os}}\right)^n \quad (4)$$

that

$$\frac{U_{ocd}}{U_{ocn}} = n \quad (5)$$

The primary photocurrent is proportional to the radiation flux (radiation power) F incident on the solar cell: $I_S = \alpha \Phi$, where α is the proportionality coefficient. Then the ratio of radiation fluxes during the day Φ_{cd} and at night Φ_{cn} is still the same

London Journal of Engineering Research

$$\frac{\Phi_{cd}}{\Phi_{cn}} = \frac{J_{cd}}{J_{cn}} = m \tag{6}$$

where from

$$J_{sd} = mJ_{sn} \tag{7}$$

where m = 40000-400000 (the illumination created by sunlight is greater than the illumination with a full Moon at night on the surface of our planet). Substitute (7) in (4)

$$\frac{J_{sd}}{J_{os}} = \left(\frac{J_{sd}}{mJ_{os}}\right)^{n} \tag{8}$$

where from

$$m^{\frac{n}{n-1}} = \frac{J_{sd}}{J_{os}} \tag{9}$$

From the formula (2), we express the ratio of currents

$$\frac{J_{sd}}{J_{os}} = e^{\frac{AqU_{ocd}}{kT}} \tag{10}$$

then

$$m^{\frac{n}{n-1}} = e^{\frac{AqU_{ocd}}{kT}} \tag{11}$$

from where n is equal to

$$n = \frac{AqU_{ocd}}{AqU_{ocd} - kT\ln m} \tag{12}$$

We find the coefficient A from the following formula

$$I_{mp} = -I_{sc}\left(1 - \frac{1}{AU_{mp}}\right) \tag{13}$$

where: U_{mp}-voltage at the point of maximum power, V; I_{mp}-current at the point of maximum power, A, V; I_{sc}-short circuit current, A.

Wherefrom

$$n = \frac{AqU_{ocd}}{AqU_{ocd} - kT\ln m} \tag{14}$$

substitute the expression (14) in (12) and get the formula for finding the number n

$$n = \frac{1}{1 - \frac{kT \ln mU_{mp}\left(1 + \frac{I_{mp}}{I_{sc}}\right)}{qU_{ocd}}} \tag{15}$$

substitute (15) in the expression (5)

$$U_{ocn} = \frac{U_{ocd}}{n} = U_{ocd} - \frac{kT \ln mU_{mp}\left(1 + \frac{I_{mp}}{I_{sc}}\right)}{q} \tag{16}$$

IV. DISCUSSION

As we can see, the obtained formula (16), the no-load voltage determines the no-load voltage at night during the day, the technical parameters of the solar cell, the temperature, and the relative illumination coefficient. We will perform the following analysis of the resulting expression. If the radiation fluxes are equal during the day and at night (m=1) the fractional part in the formula (16) turns to zero, and $U_{ocd} = U_{ocn}$, which is to be expected.

V. CONCLUSION

The work is devoted to the use of solar energy. The conclusion of the formula for calculating the no-load voltage of the solar module at night is given. The obtained result may be applicable for further engineering calculations of energy generation by solar modules.

REFERENCES

1. Ranjeva M., Kulkarni A.K. Design Optimization of Hybrid, Small, Decentralized Power Plant for Remote/Rural Areas // Energy Procedia. – 2012. – V. 20. – P. 258–270.
2. Kanareykin, A. I. On the efficiency of solar energy use in the middle zone of the Russian Federation // Problems and prospects in the international transfer of innovative technologies: Collection of articles following the results of the Interna-tional Scientific and Practical Conference. - Sterlitamak: AMI, 2021. - C.23-25.
3. Babaa S., Armstrong M., Pickert V. Overview of maximum power point tracking control methods for PV systems. Journal of Power and Energy Engineering, no. 2, pp. 59–72. DOI:10.4236/jpee.2014.28006.
4. Djeghloud H., Guellout O., Larakeb M., Bouteldja O., Boukebbous S., Bentounsi A. Practical study of a laboratory undersized grid-connected PV system. 2014 IEEE Innovative Smart Grid Technologies – Asia (ISGT ASIA), 2014, pp. 618–623. DOI: 10.1109/ISGT-Asia.2014.6873863.
5. Dolara A., Faranda R., Leva S. Energy comparison of seven MPPT techniques for PV systems. J. Electromagnetic Analysis & Applications, 2009, no. 3, pp. 152–162. DOI:10.4236/jemaa.2009.13024.
6. Dorofte C., Borup U., Blaabjerg F. A Combined two-method MPPT control scheme for grid-connected photovoltaic systems. European Conference on Power Electronics and Applications. Dresden, 2005, pp. 1–10. DOI: 10.1109/EPE.2005.219714.
7. Kanareykin A. I. On the correctness of calculating the Fill Factor of the solar module IOP Conf. Series: Earth and Environmental Science 808 (2021) 012018. DOI:10.1088/1755-1315/808/1/01 2018.

Modal Analysis of Reinforced Concrete and Fiber Reinforced Concrete Hollow Core Floor Slabs

Surianinov M.H., Murashko O.V. & Korneychuk T.S.

ABSTRACT

Analytical, experimental and numerical results of determination of natural frequencies and forms of oscillations of reinforced concrete and fiber-reinforced concrete hollow core slabs are given. The problem of determination of natural frequencies and forms of oscillations of reinforced concrete and fiber-reinforced concrete slabs at the initial modulus of elasticity is solved analytically. Computer modeling of the considered constructions in two software complexes is performed and the technique of their modal analysis on the basis of the finite element method is developed. Experimental researches of free oscillations of the considered structures are carried out and the comparative analysis of all received results is carried out. The frequency spectrum calculated by the finite element method (ANSYS) is approximately 4% lower than calculated analytically; the results of the calculation in SOFiSTiK differ by 2% from the results obtained in ANSYS; the discrepancy with the experimental data reaches 15%, and all frequencies calculated experimentally, greater than the frequencies calculated analytically or by the finite element method. The obtained frequency range of fiber concrete slabs is higher than that of concrete, which gives reason to recommend fiber reinforced concrete for the manufacture of structures that will work under dynamic influences.

Keywords: slab, concrete, fiber-reinforced con- crete, dynamic, modal analysis, oscillation freque- ncy, form of oscillation, model, finite elements method, SOFiSTiK, ANSYS.

Classification: FOR Code: 670904

Language: English

London Journals Press

LJP Copyright ID: 392982
Print ISSN: 2631-8474
Online ISSN: 2631-8482

London Journal of Engineering Research

Volume 21 | Issue 3 | Compilation 1.0

Modal Analysis of Reinforced Concrete and Fiber-Reinforced Concrete Hollow Core Floor Slabs

Surianinov M.H.[α], Murashko O.V.[σ] & Korneychuk T.S.[ρ]

ABSTRACT

Analytical, experimental and numerical results of determination of natural frequencies and forms of oscillations of reinforced concrete and fiber-reinforced concrete hollow core slabs are given. The problem of determination of natural frequencies and forms of oscillations of reinforced concrete and fiber-reinforced concrete slabs at the initial modulus of elasticity is solved analytically. Computer modeling of the considered constructions in two software complexes is performed and the technique of their modal analysis on the basis of the finite element method is developed. Experimental researches of free oscillations of the considered structures are carried out and the comparative analysis of all received results is carried out. The frequency spectrum calculated by the finite element method (ANSYS) is approximately 4% lower than calculated analytically; the results of the calculation in SOFiSTiK differ by 2% from the results obtained in ANSYS; the discrepancy with the experimental data reaches 15%, and all frequencies calculated experimentally, greater than the frequencies calculated analytically or by the finite element method. The obtained frequency range of fiber concrete slabs is higher than that of concrete, which gives reason to recommend fiber reinforced concrete for the manufacture of structures that will work under dynamic influences.

Keywords: slab, concrete, fiber-reinforced concrete, dynamic, modal analysis, oscillation frequency, form of oscillation, model, finite elements method, SOFiSTiK, ANSYS.

Author: odesa state academy of civil engineering and architecture.

INTRODUCTION

The work of reinforced concrete structures, including slabs, under static loads has been studied quite well. And the issues of plate dynamics are much less well covered. At the same time, the emphasis in research is placed on short-term loads–impulse, impact, explosion. Meanwhile, when solving almost any problem of dynamics, it becomes necessary to determine the natural frequencies and modes of vibration, since these parameters determine the behavior of the system under other types of dynamic influences.

Dynamic calculations of reinforced concrete structures are associated with solving a set of issues: determining the parameters of dynamic loads, limiting states, taking into account changes in the strength and deformation characteristics of concrete and reinforcement, determining forces and deformations in structures, etc.

The nature of reinforcement makes a significant contribution to the nature of changes in the dynamic parameters of reinforced concrete structures. This fact is well known, but has not yet been thoroughly studied, either quantitatively or qualitatively. And the influence of dispersed reinforcement, in particular, steel fiber, on the dynamic parameters has been studied even less.

Despite the growing interest in steel fiber concrete and the corresponding increase in publications, the available data are contradictory, have a certain incompleteness, which allows us to give only a general assessment of the results presented in them. So, research in this direction is relevant.

II. ANALYSIS OF PUBLICATIONS

The behavior of reinforced concrete slabs under static loads is reflected in the works [1-5]. Slabs

with dispersed reinforcement are described in [6-9]. Let us dwell on these works in more detail. So, in [6], the effect of steel fiber added to reinforced concrete slabs is studied. Four-point bending tests are carried out on six slabs to investigate the structural behavior of the slabs taking into account two different parameters – slab thickness and steel fiber volume fraction. In [7], the possibility of limiting the crack width in concrete industrial floors is studied by adding steel fiber to the mixture. In [8], a comparison of the properties of concrete slabs with two types of added fibers is presented. One sample had no fibers and served as a control. The other four had steel and polypropylene fibers added in different volumetric ratios. Interesting is the work [9], where several full-size road slabs reinforced with different volume fractions of steel fibers with different geometries at a point load in the center of the slab are studied.

The issues of plate dynamics are studied in [10-15]. Seven slabs were tested under drop load in [10]. The test results showed that the addition of steel fibers was very effective. In [11], the process of deformation and destruction of a reinforced concrete slab under the influence of an air shock wave is considered. The plate is loaded by detonating an explosive in a shock tube. Numerical modeling is carried out in the LS-DYNA package, the finite element method with an explicit time integration scheme is used.

Analysis of publications shows that the problem of determining the natural frequencies and modes of vibrations of plates is still poorly understood.

III. PURPOSE AND OBJECTIVES OF THE RESEARCH

The aim of this work is analytical, experimental and numerical determination of natural frequencies and forms of oscillations of reinforced concrete and fiber-reinforced concrete hollow core slabs.

IV. PROBLEM FORMULATION

To achieve this goal, it is necessary to solve the following tasks:

1. Analyze modern analytical, numerical and experimental methods for studying the dynamics of reinforced concrete and fiberreinforced concrete slabs.
2. Solve analytically the problem of determining the natural frequencies and modes of vibration of reinforced concrete and fiberreinforced concrete slabs.
3. Perform computer modeling of the structures under consideration and develop a method for their modal analysis based on the finite element method.
4. Carry out experimental studies of free vibrations of the structures under consideration and a comparative analysis of all the results obtained.

V. RESEARCH RESULTS

A series of models of hollow core floor slabs (Fig. 1) with reinforcing rod reinforcement class A III was made. The geometric dimensions of the model are reduced by half in relation to the dimensions of the serial slab. In this case, for technological reasons (fiber size), model plates have 5 voids, not 6, as in serial plates. At the preliminary stage of research from concrete and fiber concrete of the same mixes cubic samples of 100 × 100 × 100 mm were made and tested on compression up to destruction that allowed to establish a class of concrete (C16/20) according to norms (big filler of fraction less than 10 mm).

During the tests, different physical and mechanical characteristics of the two materials were determined, including those required for dynamic calculations. These values were used in analytical calculations and in numerical simulations.

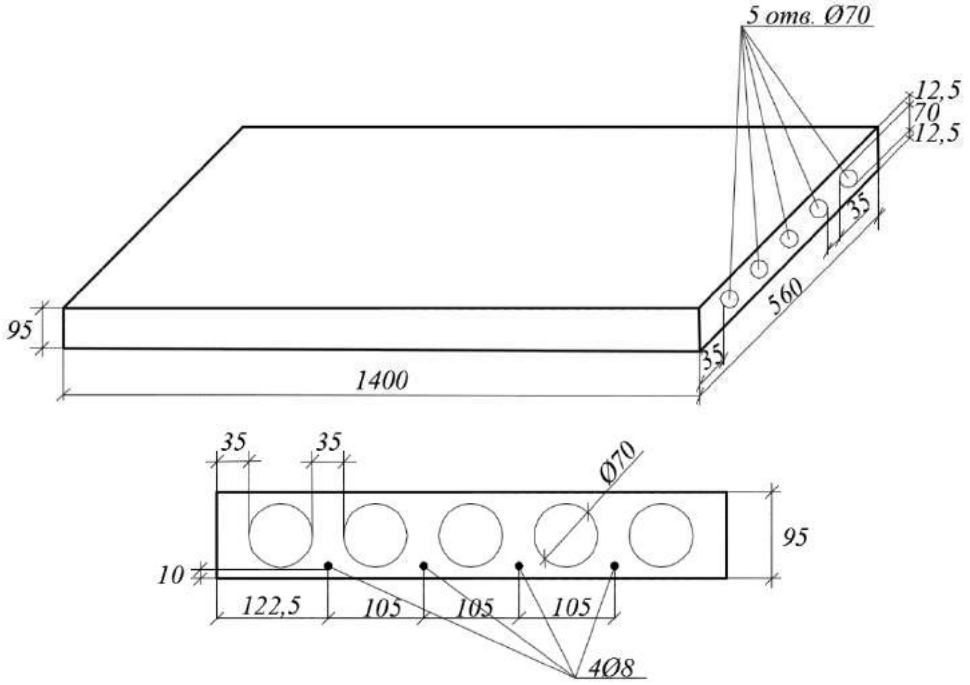

Fig. 1: Model of reinforced concrete hollow core slab

Static tests of model slabs made of reinforced concrete were carried out on a specially mounted test bench. The scheme of loading is shown in Fig. 2. In the course of these tests, the load was applied in steps of 10% of the calculated value of the destructive load.

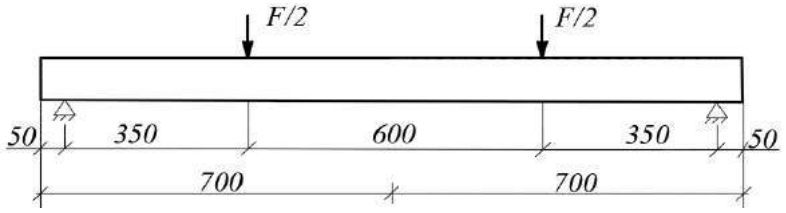

Fig. 2: Load scheme

In classical dynamics it is shown that the form of the differential equation of free oscillations under the action of a system of constant forces will be the same as in their absence, if the displacement of the body is subtracted from the position of its static equilibrium [16]. This means that in the field of elastic deformations, the natural frequency does not depend on the external static load on the structure. As a result of static tests, it was found that the process of crack formation in the plates begins at the seventh stage of loading, at a load of 16.6 kN. The fracture moment of 2.94 kNm, the same for all tested plates, was recorded here. The destructive load was 27.9 kN at the seventh stage of loading at 15.41 kNm.

Thus, the load at the beginning of the crack is approximately 0.6 of the actual value of the destructive load. Therefore, when determining the frequencies and forms of free oscillations of the reinforced concrete slab, we can assume that the deformation is elastic not only in the absence of external static load, but also when it changes in the range from 0 to 0.5 of the actual destructive load.

In the course of our work we performed analytical, computer and experimental studies of model hollow slabs (concrete and fiber-reinforced concrete) under two variants of boundary conditions - hinged support along the entire contour and hinged support on two short sides and free two other sides, as well as serial hollow slabs (concrete and fiber concrete) with hinged support on two short sides and free two other sides.

The next experiment was performed with serial multi-hollow floor slabs by conductin g full-scale static and dynamic tests in the laboratory(Fig. 3).

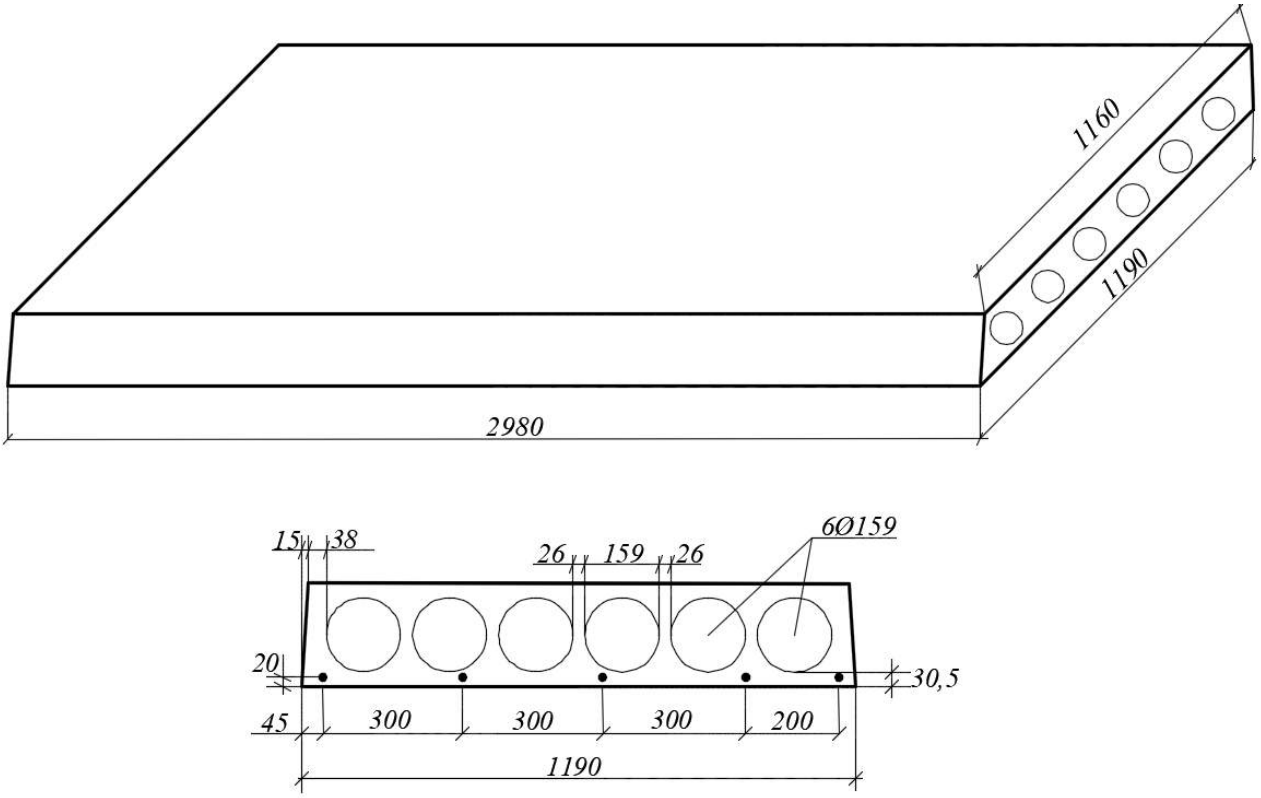

Fig. 3: Serial hollow core floor slab

Floor slabs are manufactured at the reinforced concrete plant in accordance with regulatory documents. For the manufacture of slabs used concrete C16/20 and reinforcement AIVC. Moreover, in the manufacture of one of the plates in the concrete mixture was added 1% steel anchor fiber.

The study of the strength properties of concrete was performed in the factory on samples-cubes with a rib size of 10 cm, which are tested for compression, and obtained the cubic strength corresponding to concrete C16/20. Determination of the strength of concrete under short-term loading was performed in accordance with the requirements of current regulations.

Analytically, the natural frequencies are determined by known formulas [17].

Experimental dynamic tests of the slab were carried out in the laboratory of the Department of Structural Mechanics of the Odessa State Academy of Civil Engineering and Architecture on a specially made test banch [18].

At dynamic tests for disturbance of cross oscillations the shock method possessing a number of advantages was used: simplicity of realization of the damped blow by means of the special shock device; no need to determine the logarithmic decrement of oscillations, the probability of which depends on the accuracy of the conditions of equality of the oscillatory energy supplied to the controlled structures. The impact uses an electromagnetic shock device, which is a modified to the required operating conditions contactor with a capacitive drive, the power of which can reach 600 J.

To create a damping shock, the surface of the rod in contact with the lower face of the test structure is covered with a layer of technical rubber, which reduces the duration of the transition period of the oscillating process.

The first four natural frequencies of oscillations of concrete and fibroconcrete model hollow slabs were experimentally determined in two variants of support - hinged along the entire contour (Table 1) and hinged support on two short sides with free two other sides (Table 2).

At the next stage, the first four natural frequencies of oscillations of concrete and fiber-reinforced concrete serial slabs with hinged support on two short sides with free two other sides were experimentally determined (Table 3). The natural frequencies determined experimentally are significantly higher than the theoretical ones.

Similar results were obtained by some other authors. Attempts to explain the observed difference by the fact that the analytical formulas for the frequencies of transverse oscillations take into account the moment of inertia of the rod, which in the case of rod reinforcement or dispersed reinforcement must be calculated by special methods, fail.

Table 1: Experimental and analytical values of oscillation frequencies of concrete and fiber-reinforced concrete model slabs with hinged support along the contour

Material	Frequency, s^{-1}	Experiment	Calculation	Discrepancy, %
Concrete	ω_{11}	2620,2	2347,4	10,4
	ω_{21}	3802,8	3318,8	12,7
	ω_{12}	9720,2	8418,3	13,4
	ω_{22}	10917,4	9389,6	14,0
Fiber-reinforced concrete, 1,0 %	ω_{11}	2662,6	2383,0	10,5
	ω_{21}	3854,9	3369,2	12,6
	ω_{12}	9891,3	8546,1	13,6
	ω_{22}	11109,7	9532,1	14,2

Table 2: Experimental and analytical values of oscillation frequencies of concrete and fiber-reinforced concrete model slabs with hinged support on two short sides with two free sides

Material	Frequency, s^{-1}	Experiment	Calculation	Discrepancy, %
Concrete	ω_{11}	496,6	442,5	10,9
	ω_{21}	1722,2	1498,3	13,0
	ω_{12}	2051,9	1764,6	14,0
	ω_{22}	3905,0	3323,2	14,9
Fiber-reinforced concrete, 1,0 %	ω_{11}	528,3	469,7	11,1
	ω_{21}	1824,7	1582,0	13,3
	ω_{12}	2166,7	1867,7	13,8
	ω_{22}	4111,8	3490,9	15,1

The algorithm for calculating the geometric characteristics of the so-called induced cross section is well known and is given in the numerous literature on reinforced concrete structures, however, based on the formulas of this algorithm, the effect of moment of inertia on oscillations will not be as significant as observed in the experiment. A more important explanation, in our opinion, is the incorrectness of the used dynamic model of reinforced plate. The classical dynamics of structures is known to be based on the theory of linear differential equations, and the oscillations of structures are considered in relation to the unstressed initial state.

Table 3: Experimental and analytical values of oscillation frequencies of concrete and fiber-reinforced concrete serial slabs with hinged support on two short sides with two free sides

Material	Frequency, s^{-1}	Experiment	Calculation	Discrepancy, %
Concrete	ω_{11}	245,8	222,2	9,6
	ω_{21}	844,0	742,7	12,0
	ω_{12}	1005,7	881,0	12,4
	ω_{22}	1891,9	1636,5	13,5
Fiber-reinforced concrete, 1,0 %	ω_{11}	262,4	235,9	10,1
	ω_{21}	892,0	788,5	11,6
	ω_{12}	1060,5	935,4	11,8
	ω_{22}	1997,2	1737,6	13,0

It is obvious that in the study of free and forced oscillations of reinforced concrete building structures such an approach is unsuitable because they are physically nonlinear systems. There are very few publications on the physically nonlinear dynamics of reinforced concrete structures, and the main attention is paid to methods for solving nonlinear equations of motion, and the concept of determining nonlinear terms of these equations is practically not studied. This requires experimental research and computer simulations to identify all the factors that affect the frequency spectrum.

Computer modeling and finite element modal analysis of hollow core slabs were performed in two packages – ANSYS [19] and SOFiSTiK [20]. In the tables 4–6 for the purpose of comparison the results of finite-element, experimental and analytical determination of frequencies in model and serial hollow slabs are summarized.

Table 4: Comparison of analytical, numerical and experimental values of frequencies of natural oscillations of model plates with hinged support on a contour

Slab	Frequency	ANSYS	SOFiSTiK	Experiment	Calculation
Reinforced concrete	1	2317,6	2311,6	2620,2	2347,4
	2	3300,8	3289,4	3802,8	3318,8
	3	8377,6	8357,8	9720,2	8418,3
	4	9309,0	9219,1	10917,4	9389,6
	5	12749,6	12359,8	Not determined	
Fiber-reinforced concrete	1	2353,0	2341,1	2662,6	2383,0
	2	3349,2	3329,7	3854,9	3369,2
	3	8506,3	8486,6	9891,3	8546,1
	4	9482,7	9372,1	11109,7	9532,1
	5	12819,2	12404,1	Not determined	

Table 5: Comparison of natural frequencies of model plates with hinged support on two sides

Slab	Frequency	ANSYS	SOFiSTiK	Experiment	Calculation
Reinforced concrete	1	427,5	423,1	496,6	442,5
	2	1441,2	1430,7	1722,2	1498,3
	3	1714,1	1675,9	2051,9	1764,6
	4	3233,9	3145,4	3905,0	3323,2
	5	6749,6	6459,8	Not determined	
Fiber-reinforced concrete	1	451,7	446,7	528,3	469,7
	2	1531,6	1520,3	1824,7	1582,0
	3	1817,1	1769,1	2166,7	1867,7
	4	3398,6	3307,4	4111,8	3490,9
	5	6819,2	6504,1	Not determined	

Table 6: Comparison of natural frequencies of serial plates with hinged support on two sides

Slab	Frequency	ANSYS	SOFiSTiK	Experiment	Calculation
Reinforced concrete	1	218,6	216,6	245,8	222,2
	2	732,2	726,4	844,0	742,7
	3	868,4	860,1	1005,7	881,0
	4	1596,3	1579,1	1891,9	1636,5
	5	3749,6	3689,1	Not determined	
Fiber-reinforced concrete	1	231,1	229,1	262,4	235,9
	2	777,7	779,7	892,0	788,5
	3	921,1	912,6	1060,5	935,4
	4	1697,2	1662,1	1997,2	1737,6
	5	3789,2	3724,4	Not determined	

The above results of calculations were obtained at the initial modulus of elasticity, i.e. correspond to the state of the plates without external load.

VI. CONCLUSIONS

Despite the fact that both software packages (SOFiSTiK and ANSYS) implement the finite element method, the process of solving the problem in each of them has its own characteristics, which slightly, but still affect the result. The main ones are: first, different finite elements are involved in different programs; secondly, the processes of construction of a finite-element mesh differ and, as a consequence, the number of finite elements with the same geometric model of the structure.

A comparative analysis of all obtained theoretical, experimental and computer results showed the following:

- The frequency spectrum calculated by the finite element method (ANSYS) is approximately 4% lower than calculated analytically;
- The results of the calculation in SOFiSTiK differ by 2% from the results obtained in ANSYS;
- The discrepancy with the experimental data reaches 15%, and all frequencies calculated experimentally, greater than the frequencies calculated analytically or by the finite element method.

The obtained frequency range of fiber-reinforced concrete slabs is higher than that of concrete, which gives reason to recommend fiber-reinforced concrete for the manufacture of structures that will work under dynamic influences.

REFERENCES

1. Golyshev, A. B., Bachinsky, V. Ya. Polishchuk, V. P., Kharchenko, A. V., Rudenko, I. V. (199-0). Design of reinforced concrete structures. Reference book. Kiev: Budivelnik. [in Russian]
2. Borovskikh, A. V. (2004). Calculations of reinforced concrete structures by limiting states and limiting equilibrium. M.: Publishing house ASV. [in Russian].

3. Fanella, D. (2015). Reinforced Concrete Structures: Analysis and Design. Second Edition. New York.
4. Karpyuk, V. M., Kostyuk, A. I., Semina, Yu. A. (2018). General Case of Nonlinear Deformation-Strength Model of Reinforced Concrete Structures. Strength of Materials, USA, 50(3). 453 – 464.
5. Oikonomou-Mpegetis, S. (2014). Behaviour and Design of Steel Fibre Reinforced Concrete Slabs. Structural Engineering Research Group. Department of Civil and Environmental Engineering. Imperial College London. London: SW7 2AZ.
6. Baarimah, A. O., Syed Mohsin, S. M. (2017). Behaviour of Reinforced Concrete Slabs with Steel Fibers. The Electronic Library, 271 0102099,doi:10.1088/1757-899X/271/1/012099.
7. Labib, W., Eden, N. (2006). An Investigation into the Use of Fibres in Concrete Industrial Ground-Floor Slabs. School of the Built Environment, Liverpool: Liverpool John Moores University. 466 – 477.
8. Hadi, Muhammad N. S. (2008). Behaviour of fibre reinforced concrete slabs. London: Francis Taylor. 407 – 412.
9. Sorelli, L. G., Meda, A., Plizzari, G. A. (2006). Steel Fiber Concrete Slabs on Ground: A Structural Matter. ACI Structural Journal: Technical Paper. Title no. 103-S58. 551 – 558.
10. Hrynyk, T. D., Vecchio, F. J. (2014). Behavior of Steel Fiber-Reinforced Concrete Slabs under Impact Load. ACI Structural Journal: Technical Paper. Title no. 111-S103. 1213 – 1224.
11. Gertsik, S. M., Novozhilov, Yu. V., Mikhalyuk, D. S. (2020). Numerical modeling of the dynamics and strength of a reinforced concrete slab under the influence of an air blast wave. Computational Continuum Mechanics. 13(3), 298 – 310. doi.org/10.7242/1999-6691/2020.13.3.24. [in Russian].
12. Aboshio, Aaron. (2015). Reinforced Concrete Slab under Static and Dynamic Loadings. At: Holiday Inn, Wembley, London. 17 (12) 1074 – 1079.
13. Kumpyak, O. G., Kopanitsa, D. G. (2002). Strength and deformability of reinforced concrete structures under short-term dynamic loading. Tomsk: Publishing house STT. [in Russian].
14. Hexin, Jin, Hong, Hao, Wensu, Chen, Cheng, Xu (2021). Spall Behaviors of Metaconcrete: 3D Meso-Scale Modelling. International Journal of Structural Stability and Dynamics. 21 (09). https://doi.org/10.1142/S0219455421501212.
15. Manuel, M. (2011). Dynamic behavior of reinforced concrete. London: Department of Civil, Geomatic & Environment Engineering .
16. Bezukhov, N. I., Luzhin, O. V., Kolkunov, N. (1987). Stability and dynamics of structures. M.: Higher school. [in Russian].
17. Vasylenko, M. V., Alekseychuk, O. M. (2004). Theory of oscillations and stability of motion K.: Higher school. [in Ukranian].
18. Surianinov, M. H., Makovkina, T. S. (2019). Experimental studies of free oscillations of reinforced concrete and fibroconcrete beams. ODABA Bulletin: Collection of Scientific Papers.74. 75 – 81. [in Russian].
19. Lazareva, D. V., Soroka, M. M., Shilyaev, O. S. (2020). Techniques of working with ANSYS PC when solving mechanics problems. Edited by M.H. Surianinova: monograph. Odessa: ODABA. [in Ukranian].
20. Kukhtin, V. N. Bulaev, I. V. Baranov I. S. (2015). Application of the SOFiSTiK calculation complex for calculation of bridge designs: the textbook. M.: MADI. [in Russian].

Preparation of High Surface Area Activated Carbon from Native Rice Husk

M. U. Muhammad, B. A. Hadi , B. Idris & M. M. Abduljalil

Usmanu Danfodiyo University

ABSTRACT

Several streams of agricultural residue is produced during agricultural activity. Activated carbon is a highly porous carbon material that is known to have good adsorption capacity. Rice husk, due to its high cellulose and lignin content, can be used to prepare activated carbon. The potential of rice husk was studied for the production of highly surface area activated carbon. The activated carbons were prepared via chemical activation with phosphoric acid and zinc chloride to identify the most suitable activating agent. The obtained activated carbons were characterized using scanning electron microscopy, BET surface area, and energy dispersive spectrometry (EDS). Phosphoric acid activation produced activated carbon with the highest porosity and surface area (427.154m^2/g) compared to that by zinc chloride activation. Carbon was the most dominant element observed in the prepared activated carbons, with the highest percentage of 85.67 % was shown by phosphoric acid activation.

Keywords: rice husk; activated carbon; chemical activation.

Classification: FOR Code: 091599

Language: English

London Journals Press

LJP Copyright ID: 392983
Print ISSN: 2631-8474
Online ISSN: 2631-8482

London Journal of Engineering Research

Volume 21 | Issue 3 | Compilation 1.0

Preparation of High Surface Area Activated Carbon from Native Rice Husk

M. U. Muhammad[α], B. A. Hadi[σ], B. Idris[ρ] & M. M. Abduljalil[Ꞷ]

ABSTRACT

Several streams of agricultural residue is produced during agricultural activity. Activated carbon is a highly porous carbon material that is known to have good adsorption capacity. Rice husk, due to its high cellulose and lignin content, can be used to prepare activated carbon. The potential of rice husk was studied for the production of highly surface area activated carbon. The activated carbons were prepared via chemical activation with phosphoric acid and zinc chloride to identify the most suitable activating agent. The obtained activated carbons were characterized using scanning electron microscopy, BET surface area, and energy dispersive spectrometry (EDS). Phosphoric acid activation produced activated carbon with the highest porosity and surface area (427.154m²/g) compared to that by zinc chloride activation. Carbon was the most dominant element observed in the prepared activated carbons, with the highest percentage of 85.67 % was shown by phosphoric acid activation.

Keywords: rice husk; activated carbon; chemical activation.

Author α σ ρ: Department of Chemistry, Shehu Shagari College of Education, Sokoto Nigeria.
Ꞷ: Central Advance Science Laboratory Complex, Usmanu Danfodiyo University, Sokoto-Nigeria.

I. INTRODUCTION

Agricultural activity is one of the occupational practices in most of sub - Saharan Africa. As a result, huge amount of waste products are generated yearly, which could be potent resources for sustainable energy sources (Yakovlev *et al.,* 2015). The high interest in a bio - based economy has stimulated a fast growing research and development on the biomass conversion techniques (Gabriele *et al.,* 2011). Activated carbon production from agricultural waste as possible economic and environmental effects. Activated carbons are used for the conversion of agricultural waste to adsorbents to remove organic chemicals, heavy metals from water which are of economic importance. Production of activated carbon from waste agricultural residue will minimize its importation (Ekpete *et al.*, 2016).

Latest developments in the preparation of carbon electrodes using several biomass residues for use in energy storage devices, such as batteries and supercapacitors are recently embraced by scientist as well researchers. The biomass residues usage as the primary precursor for the production of carbon electrodes has been increasing over the last years due to it being a renewable source with comparably low processing cost, providing prerequisites for a process that is economically and technically sustainable (Simões dos Reis *et al.*, 2020).

Liu *et al.* (2015) prepared highly surfaced-area activated carbon from coconut shells using KOH as activating agent. The activated carbon was used as a battery cathode. Similarly, Osman *et al.* (2016) synthesized activated carbon using different parts (shaggy and core) palm oil empty fruit bunch through the physical activation (at temperature of 600, 700, and 800°C). The result showed that the highest yield for activated carbon was achieved at 700°C. Dieu *et al.* (2020) prepared activated carbon for high - performance supercapacitors using oil palm empty fruit bunches (EFBs), through series of cleaning, carbonization and chemical activation processes. The activated carbon has a specific surface area of 2774 m²/g, which is very high among AC synthesized from the biomass materials. The specific capacities of AC and nitrogen-doped AC are found to be 182 and 217 F/g, respectively. This

was determined at the current density of 0.5 A/g using 6M KOH as aqueous electrolyte.

Optimization of Activated carbon preparation from Palm empty fruit bunch fiber process was studied by Arshad *et al.* (2019) using RSM-design under CO_2 atmosphere where the effect carbonization temperature and time were studied. The maximum I_2 adsorption of 373.41 mg/g with surface area (BET) of 1.09 m^2/g was observed at the end of the study. The results show that optimal carbonization condition for the process is achieved at 450°C for 90 min. Also maximum I_2 adsorption of 841.32 mg/g was achieved. The BET surface area of 900.02 m^2/g also was achieved. The activated carbon percentage yield of 49.33% was obtained at 500°C carbonization temperature by Hanum *et al.* (2017) from dried rice husk carbonized from 400 to 600°C different temperature under constant nitrogen atmosphere. After that, the carbon was treated with hydrochloric acid.

Activated carbon production was done mainly via two routes; first, through carbonization of the biomass under inert or oxidized condition. Second, through physical activation or chemical activation at lower temperature which gave a better quality of porous structure ACs and lower energy costs (Ioannidou and Zabaniotou, 2007). Prahas *et al.* (2008) reported that widely used chemical reagents for activation are $ZnCl_2$, NaOH, H_3PO_4, and metal chemicals (e.g., KOH and K_2CO_3). This Chemical activation is a commonly used method as reported in the literature (Lillo-Ródenas *et al.,* 2003; Kalderis *et al.*, 2008 and Adinata *et al.*, 2007). A high surface area up to 700~2000 m^2/g activated carbon is expected when the biomass waste is used as feedstock and chemical activation a production method. The properties of the obtained carbon materials strongly depend on the structure determined by the type of starting material, activating agent, and process conditions (Hesas *et al.,* 2013).

Presently, researchers are searching for an alternative and benign approach to producing the most low-cost activated carbon as an inexpensive adsorbent for the treatment of wastewater from industrial waste. This study intends to determine the potentials of native rice husk samples to prepare activated carbons using Phosphoric acid and Zinc chloride as activating agents.

II. METHODOLOGY

2.1 Sample Collection and Treatment

Sample was procured from the Attajiri rice mill at Kware local government area, Sokoto. The AOAC (1999) analyses methods (with amendment) were employed to obtain a required sample for these analyses. The collected sample was washed with distilled water to remove debris, dust, and other impurities and then dried in a hot air circulating oven at 105˚C overnight to remove moisture. The dried sample was ground into powdered and sieved to a size of 4mm. Standard procedures were employed for the preparation of solutions and other reagents using deionized water.

2.2 Preparation of Activated Carbon

The activated carbons were prepared following a method described by Anisuzzaman *et al.* (2015) with some amendments. The dried rice husk sample was impregnated directly with H_2PO_3 reagent and labeled RHP, while impregnation with $ZnCl_2$ was labeled RHZ. After the soaking, the samples were kept for 72hrs with constant shaking to ensure sufficient absorption of the reagents. Then it was filtered and dried in an oven at 110°C overnight. After that the dried sample was semi carbonized in a Muffle furnace for 15 minutes at 200°C and then heated to a temperature of 500°C for 45 minutes.

After the chemical activation, the activated carbon was refluxed with distilled water for 3h at a temperature of 80°C to remove excess reagent. Then, reflux was repeated several times until the constant pH value was achieved. The activated carbon prepared was refluxed with 0.1M HNO_3 for 1h to remove heavy metals and ash.

2.3 Characterization of Activated Carbon

The activated carbons prepared were characterized using surface Analyzer and Scanning Electron Microscope to determine micropore size, micropore volume, BET surface area, and morphological properties of the carbons.

2.4 Morphology and Elementals composition of the activated carbon

Scanning Electron Microscope (SEM) was used to observe the surface morphology and porosity of the activated carbons. The SEM images of the activated carbon prepared were taken using JEOL JSM-5000V Scanning Electron Microscope. The EDS analysis was carried out for elemental composition of the samples determine.

2.5 Surface Analyses of the Activated Carbon

The surface area and pore volume of the Activated Carbons (AC) were determined using Quantachrome Instrument (Version 11.03) by N_2 adsorption isotherms at 77.35K. The AC were degassed prior to the analysis for 3 hours at 250 ^{0}C in a vacuum. The surface area was determined using Multipoint Brunauer-Emmett-Teller (BET) method, while pore volume and pore size were estimated by application of the Barrett-Joyner-Halenda (BJH) method. The DR method was used to determine micropore (S_{mi}) surface area.

III. RESULTS AND DISCUSSION

3.1 Porous Properties of the Activated Carbon

Table 1: Activated Carbon Porous properties

Sample	S_{BET}(m^2/g)	S_{mi}(m^2/g)	S_{mi}/ S_{BET}	S_{mi}/ S_{BET} (%)
RHZ	362.315	390.237	1.077	107.7
RHP	427.154	428.802	1.003	100.3

The porous properties of the prepared AC from rice husk are presented in Table 1. The BET surface area for RHZ is 362.315m^2/g and 427.154m^2/g RHP. As evident from the table, phosphoric acid activation gives a high surface and pore volume (Figure 1). Phosphoric acid-treated activated carbon showed approximately 8% higher BET surface area than Zinc chloride treated activated carbon. The creation of pores in the carbon may be attributed to the release of volatiles from the biochar on carbonation. The H_3PO_4 reacting within the cellulose structure is assumed to have induced an enhancement of the pore volume (Benadjemia *et al.*, 2011).

The pore size distribution is an important clue revealing the adsorption mechanisms of porous substances. Figure 2 shows the pore size distribution of the rice activated carbon. The pores of adsorbing material were divided into three categories; micropore (diameter < 2 nm), mesopopore (2–50 nm), and macropore (>50 nm) (Ryu *et al.,* 1999). It could be seen from (Figure 2) that rice husk AC has narrow pore size distributions, including both micropores and mesopores. Most pores of activated carbons were composed of mesopores with sizes ranging from 2 – 2.8 nm. ACs also contained micropores with narrow range from 1.7 to 1.9nm. The shared porosity in the activated carbon was approximately 63.6% and 36.4%, mesopore and micropore sizes, respectively.

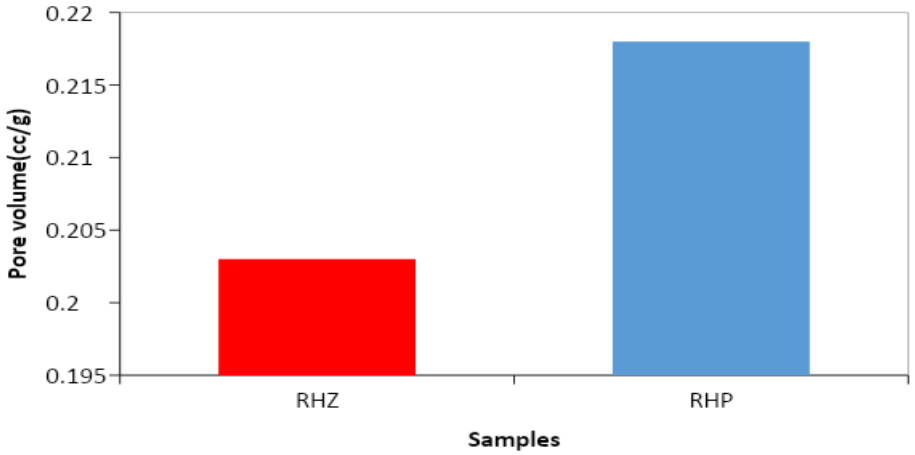

Figure 1: Pore size distribution of the activated carbons

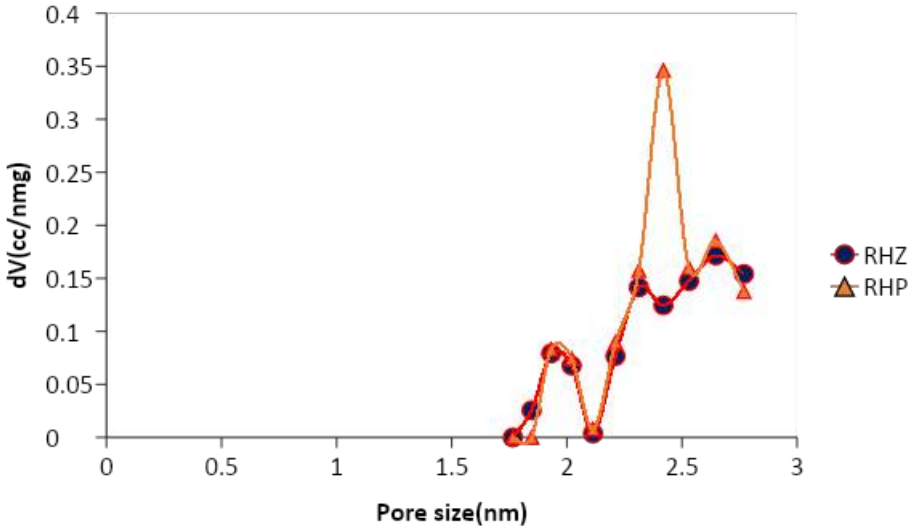

Figure 2: Pore size distribution of the activated carbons

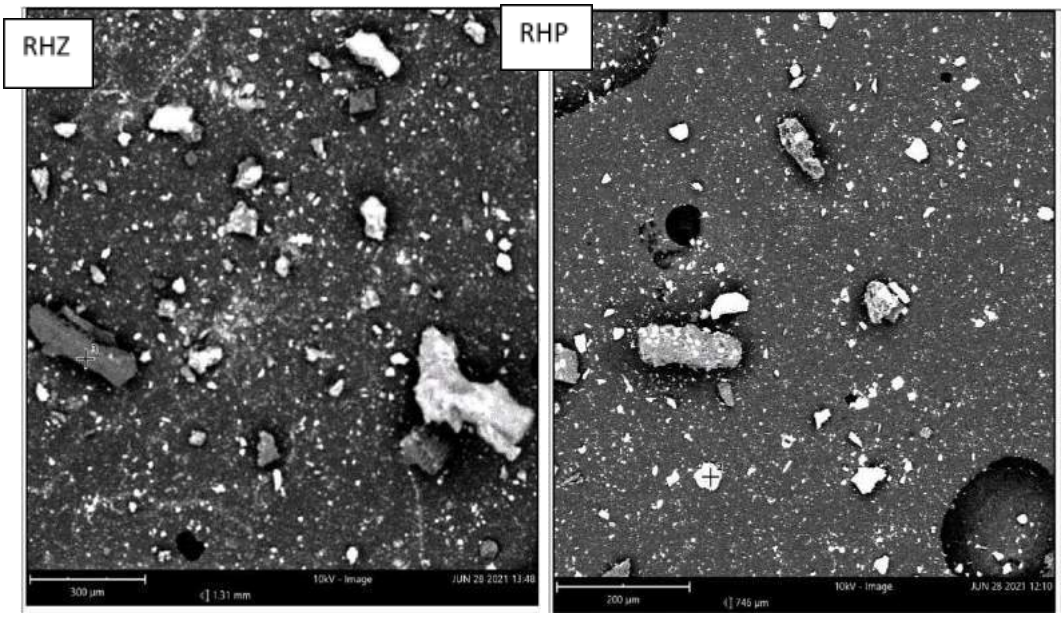

Figure 3: Scanning Electron Microscope (SEM) micrographs for ACs

Scanning electron microscopy (SEM) is an instrument for surface studies of adsorbents (Aljeboree *et al.*, 2017). It can also be used in the characterization of activated carbon. Evidence of porosity could be observed from the SEM images. The porosity was due to the decomposition of lignin, cellulose, and hemicellulose during carbonization, resulting in micropores and mesopores. The SEM structure in Figure 3 indicated that the porous structures were obtained on the activated carbons via chemical activation with $ZnCl_2$ and H_2PO_3. Also, it was observed that the surfaces of the activated carbon possess irregular circular pore structures and aggregation in different sizes and shapes. Phosphoric acid activation shows a better-cleared surface area compared to zinc chloride activation process. A well-clear surface of activated carbon may be attributed to the removal of impurities and volatile substances during activation. The presence of these porous structures implies the potential use of the prepared carbons as catalyst support because such pores provide sites on which active materials could be adsorbed to form an active catalyst

Table 2: Elemental Composition of the activated carbon

Sample	Carbon	Oxygen
RHP	85.67	14.33
RHZ	68.35	31.65

Elemental components of the prepared activated carbon presented in the Table 2 and EDS spectra (Fig. 4 & 5). Phosphoric acid-derived activated carbon (RHP) has a high carbon content of 85.67% and low oxygen content of 14.33 % compared to 68.35% and 31.65% for zinc chloride-derived activated carbon (RHZ). This indicates that phosphoric acid performs better as an activating agent than zinc chloride. This is also evident from the SEM image of RHP, which shows a better porous structure than RHZ.

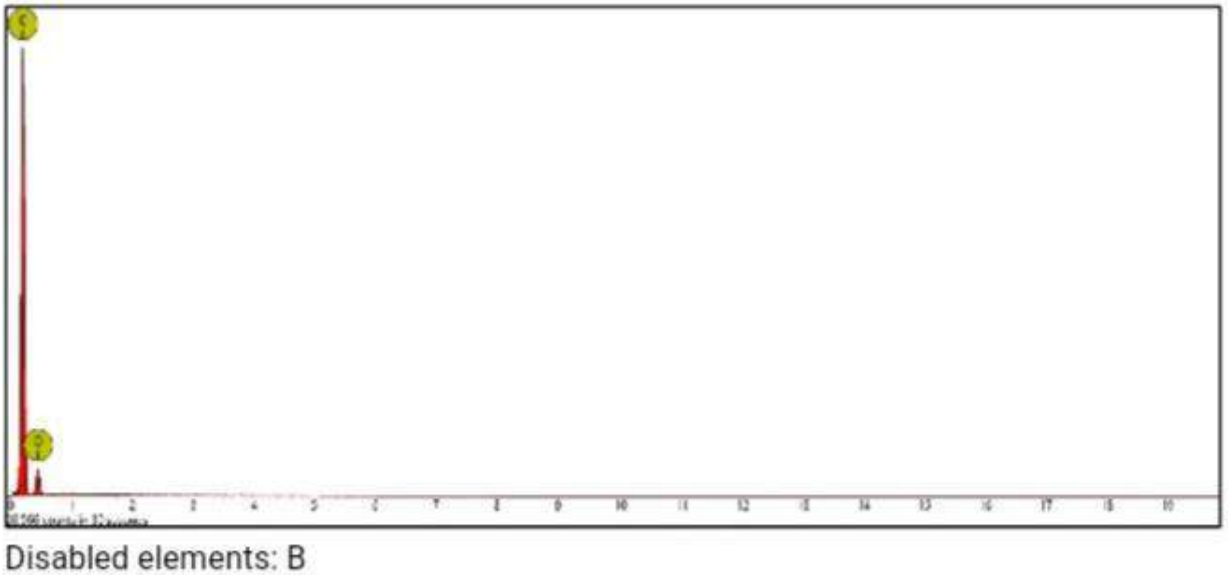

Figure 4: EDS spectra of RHP activated carbon

ACKNOWLEDGEMENTS

The authors are grateful to the Tertiary Education Trust Fund (TETFUND) for funding this research through IBR 2013/2014/2015 merged interventi on.

IV. CONCLUSIONS

The present research studies compare phosphoric acid and zinc chloride as activation agents for the preparation of activated carbon from rice husk. The results show that AC prepared from Phos-

phoric acid activation has a higher surface area, percentage carbon, and better porosity compared to Zinc chloride activation. The results established that the development of porosity in the prepared carbons can be affected by two different agents. From this study it is evident that pore size distributions of the activated carbon could be achieved when different type of activation reagent are used.

REFERENCES

1. Adinata D, Daud, W. (2007). Preparation and characterization of activated carbon from palm shell by chemical activation with K_2CO_3. *Bioresource Technology* **98** (1):145–149.
2. Aljeboree, A. M., Alshirifi, A. N., & Alkaim, A. F.(2017). Kinetics and equilibrium study for the adsorption of textile dyes on coconut shell activated carbon. *Arabian journal of chemistry*, ***10***, S3381-S3393.
3. AOAC, (1999). Offiacial method of Analysis of the Association of Analytical Chemistry. Hauwist, W. (Ed), 14th Edition.
4. Anisuzzaman, S. M., Joseph, C.G., Ashri Bin Wan Daud, W. M. Krishnaiah, D. and Yee, H. S. (2015) Preparation and characterization of activated carbon from Typha orientalis leaves. *International Journal Industrial Chemistry* **6**:9-21 DOI 10.1007/s40090-014-0027-3.
5. Arshad, S. M, Ngadi, N., Wong, S., Amin, N. S., Razmi, F. A. and Mohamed, N B. Inuwa, I. M., Aziz, A. A. (2019) Optimization of phenol adsorption onto biochar from oil palm empty fruit bunch (EFB) *Malaysian Journal of Fundamental and Applied Sciences* ***15*** (1): 1-5.
6. Benadjemia, M., Millière, L., Reinert, L., Benderdouche, N., & Duclaux, L. (2011). Preparation, characterization and Methylene Blue adsorption of phosphoric acid activated carbons from globe artichoke leaves. *Fuel Processing Technology*, **92**(6), 1203-1212.
7. Dieu, H. T., Charoensook, K., Tai, H. Lin, Y. and Li. Y. (2020) Preparation of activated carbon derived from oil palm empty fruit bunches and its modification by nitrogen doping for supercapacitors. *Journal of Porous Materials* https://doi.org/10.1007/s10934-020-00957-2.
8. Ekpete, O. A., Marcus, A. C. and Osi, V. (2017) Preparation and Characterization of Activated Carbon Obtained from Plantain (*Musa paradisiaca*) Fruit Stem *Hindawi Journal of Chemistry*: 1-6 https://doi.org/10.11 55/2017/86 35615.
9. Girio, F. M., Fonseca C., Carvalheiro F., Duarte L. C., Marques, S. and Bogel-Lukasik R., (2010) *Bioresources Technology*, **101**, 4775 – 4800.
10. Hanum, F. B. and Wirani, L. I. (2017) Characterization of Activated Carbon from Rice Husk by HCl Activation and Its Application for Lead (Pb) Removal in Car Battery *IOP Conference Series: Materials Science and Engineering* **180** 012151.
11. Hesas R. H, Daud, A.W., Sahu, J. N. and Arami-Niya, A. (2013). The effects of a microwave heating method on the production of activated carbon from agricultural waste: a review. *Journal of Analytical Applied Pyrolysis* **100**:1–11. https://doi.Org/10.1016/j.jaap.2012.12.019.
12. Ioannidou, O. and Zabaniotou, A. (2007). Agricultural residues as precursors for activ- ated carbon production: a review. *Renewable Sustainable Energy Revision* **11**(9):1966–2005.
13. Kalderis, D. and Bethanis, S. (2008). Production of activated carbon from bagasse and rice husk by a single-stage chemical activation method at low retention times. *Bioresource Technology* **99**(15):6809–6816.
14. Liu, M., Chan, Y., Chen, K., Zhang, N. Zhao, X. and Zhao, F., Dou, Z., He, X. and Wang, L. (2015) Activated carbon for Li-S batteries, *Bio Reseources* **10** (1): 155-168.
15. Lillo-Ródenas MA, Cazorla-Amorós, D.(2003) .Understanding chemical reactions between carbons and NaOH and KOH: an insight into the chemical activation mecha- nism. *Carbon* 41(2):267–275 .
16. Nda-Umar U. I., Ramli, I. Muhamad, E. N., Taufiq-Yap, Y. and Azri, N. (2020) Synthesis and characterization of sulfonated carbon cata- lysts derived from biomass waste and its evaluation in glycerol acetylation *Biomass Conversion and Biorefinery* https://doi.org/10.1007/s13399-020-00784-0.

17. Ryu, K. H., and Haile, S. M. (1999). Chemical stability and proton conductivity of doped BaCeO3–BaZrO3 solid solutions. *Solid State Ionics*, ***125***(1-4), 355-367.
18. Simões dos Reis, G., Larsson, S. H., Pequeno de Oliveira, H. Thyrel, M. and Lima, E.C. (2020) Sustainable Biomass Activated Carbons as Electrodes for Battery and Super- capacitors —A Mini-Review *Nanoma- terials* 10, (1398): 1-24.
19. Prahas, D and Kartika Y. (2008) Activated carbon from jackfruit peel waste by H_3PO_4 chemical activation: pore structure and surface chemistry characterization. *Chemical Engineering Journal* **140**(1–3):32–42
20. Yakovlev, V.A., Khromova, S.A., Sherstyuk, O.V., Dundich, V.O., Ermakov, D.Y., Novopashina, V.M., Levedev, M.Y., Bulavchenko, O., Parmon, V.N. (2009) Development of New Catalytic Systems for Upgrade of bio-fuels production from bio-crude-oil and biodiesel, *Catalysis Today,* **144:** 362-366.

This page is intentionally left blank

Composition and Characterization of Wood Vinegar Extracted from Coconut Shell and Coconut Wood

Aljon Victor G. Nibalvos, Neil Alejandro A. Pinarok & Grace O. Manlapas

Eastern Samar State University

ABSTRACT

Coconut wood and coconut shell were subjected to destructive distillation to extract wood vinegar which can be utilized in agriculture, livestock farming, and even in the pharmaceutical industry. This study is centered on determining the physical and chemical characteristics of wood vinegar extracted from two different organic samples. Qualitative and Quantitative Analytical processes were used to determine the composition and characteristics of wood vinegar from coconut wood and coconut shell. Results indicate that wood vinegar from coconut wood is orange to dark orange in color while yellowish to dark yellow was observed on coconut shell wood vinegar.The odors of the wood vinegars coming from the 2 samples were the same, according to most respondents which was copra-like odor. pH indicates high acidity on both samples and miscibility to most polar substances.

Keywords: coconut shell, coconut wood, wood vinegar, chemical properties, chemical composition.

Classification: FOR Code: 070199

Language: English

London Journals Press

LJP Copyright ID: 392985
Print ISSN: 2631-8474
Online ISSN: 2631-8482

London Journal of Engineering Research

Volume 21 | Issue 3 | Compilation 1.0

Composition and Characterization of Wood Vinegar Extracted from Coconut Shell and Coconut Wood

Aljon Victor G. Nibalvos[α], Neil Alejandro A. Pinarok[σ] & Grace O. Manlapas[ρ]

ABSTRACT

Coconut wood and coconut shell were subjected to destructive distillation to extract wood vinegar which can be utilized in agriculture, livestock farming, and even in the pharmaceutical industry. This study is centered on determining the physical and chemical characteristics of wood vinegar extracted from two different organic samples. Qualitative and Quantitative Analytical process were used to determine the composition and characteristics of wood vinegar from coconut wood and coconut shell. Results indicate that wood vinegar from coconut wood is orange to dark orange in color while yellowish to dark yellow was observed on coconut shell wood vinegar. The odors of the wood vinegars coming from the 2 samples were the same, according to most respondents which was copra-like odor. pH indicates high acidity on both samples and miscibility to most polar substances. Total Acid Content indicates a slightly higher percentage for coconut wood than coconut shell. Small amounts of soluble tar were observed on the two wood vinegar samples which indicates a high degree of purity and the moisture for coconut wood is lower than the coconut shell. Phenolic compounds were mostly characterized in the wood vinegar from the two samples with an almost similar composition but with varying concentrations, also, other trace chemicals were found on the wood vinegar samples indicating the complexity and varied uses of wood vinegar in different fields of agriculture and pharmaceuticals. It is therefore recommended that a pilot medium scale production of wood vinegar from coconut shell and coconut wood be conducted for agricultural and livestock use.

Keywords: *coconut shell, coconut wood, wood vinegar, chemical properties, chemical composition.*

Author α: Instructor, College of Arts and Sciences, Eastern Samar State University, Borongan City.
σ: Head, Tourism Department, Eastern Samar Provincial Capitol, Borongan City.
ρ: Director, International Linkaging, Eastern Samar State University, Borongan City.

I. BACKGROUND OF THE STUDY

A recent trend in agricultural chemistry and green chemistry which is now utilized by some farmers in Southeast Asia is the Wood Vinegar. Wood vinegar comes from the destructive distillation of wood, wood tar and charcoals are also one of the products of this type of process involving wood.

Wood vinegar is produced when smoke from charcoal production is cooled by outside air while passing through a chimney or flue pipe. The cooling effect causes condensation of pyroligneous liquor, particularly when the temperature of smoke produced by carbonization ranges between 80 and 180°C (Nikhom, 2010 as cited by ECHO, 2012). This temperature is reached at the carbonization stage of exothermic decomposition and is indicated by the production of yellowish, acrid smoke (ECHO, 2012).

According to Payamara, J. (2011) wood vinegar production is a development of traditional process of charcoal burning or the burning of wood in an airless condition reducing it to a charcoal rather than a carbon dioxide, water vapor of firebricks is substituted for the mound of earth, and a device is added to collected and cool the vapors released to condense them.

Current research on wood vinegar states that it has beneficial effects to plants, soil and even on animal diet. Wood vinegar is made as an alternative to some mixture fertilizers which further contain numerous poisons that attach to plants and retain to the soil contaminating it.

Moreover, in the process of wood vinegar, there is only small information regarding the use of coconut shell and its trunk as a source of wood vinegar, hence this study will be conducted, which will in turn give additional source of wood vinegar, not only from true trees, but also from coconut tree.

II. OBJECTIVES OF THE STUDY

This research extracted wood vinegar from coconut shell and coconut trunk as a newer source of wood vinegar. Specifically, this study answered the following:

1. Determine the physical property of the coconut shell and trunk wood vinegar in terms of:
   a. Color
   b. Miscibility
   c. Odor
   d. pH
2. Determine the composition of wood vinegar generated from coconut shell and coconut wood in terms of:
   a. Acid content
   b. Water Content
   c. Soluble Tar Content
3. Determine the present Basic and Neutral substances in the wood vinegars.

III. METHODOLOGY

3.1 Research Design

This experimentally designed study focused on the extracting wood vinegar from coconut shell and wood which is basically used as fuel, and further determined its physical and chemical compositions of the extracted wood vinegar.

3.2 Preparation of Materials

Coconut shells and were collected from Borongan city market. Whereas, coconut wood was collected from the vicinity of Eastern Samar State University, Borongan City. The said components were then coursing and drying it in an open space to exclude water molecules from the samples and readied for destructive distillation.

3.3 Instrument and Data Gathering procedure

Dry distillation of wood was done using procedures from Phywe (2017). The dry distillation (as seen on Figure 1) was assembled by the researchers for a faster rate of extracting wood vinegar. Experimental procedures were done under laboratory conditions, all in triplication to minimize errors. Extra care was also utilized in this experiment for explosive and toxic fumes are emitted during distillation.

Figure 1: Kiln for Extracting Wood Vinegar

3.4 Instruments of the Study

In the following figure (Figure 2) the instruments and reagents that were used in the study are specified:

Position No.	Material	Order No.	Quantity
1	Support rod, stainless steel, l=370 mm, d=10 mm	02059-00	1
2	Support base, variable	02001-00	1
3	Glass beaker DURAN®, short, 250 ml	36013-00	1
4	Test tube rack for 12 tubes, holes d= 22 mm, wood	37686-10	1
5	Boss head	02043-00	2
6	Glass tube,right-angled w.tip,10	36701-53	(1)
7	Protecting glasses, clear glass	39316-00	1
8	Rubber stopper, d = 22/17 mm, 1 hole	39255-01	2
9	Universal clamp	37715-00	2
10	Glass tubes,right-angled, 10	36701-59	(1)
11	Pipette with rubber bulb	64701-00	1
12	Rubber tubing, i.d. 6 mm	39282-00	1
13	Test tube, 180x18 mm,100pcs	37658-10	(1)
14	Test tube,180x20 mm,side arm,PN19	36330-00	1
15	Spoon, special steel	33398-00	1
16	Test tube,180x20 mm,DURAN, PN19	36293-00	1
	Butane burner f.cartridge 270+470	47536-00	1
	Butane catridge CV 300 Plus, 240 g	47538-01	1
	Glycerol, 250 ml	30084-25	1
	Sodium chloride 1000 g	30155-70	1
	Iron wool 200 g	31999-20	1
	Wood splints, package of 100	39126-10	1
	Indicator paper, pH1-14, roll	47004-02	1

Figure 2: Equipment and Reagents used in Dry distillation

3.5 Physical and Chemical Characterization

After extraction, the wood vinegar collected was placed in a dry opaque polyethylene (PET) bottle and placed standing for 24 hours to settle. Once this is achieved, the clear liquid (wood vinegar) from the crude extract was separated by pipetting off to exclude foreign chemicals which may interfere with the results. The pure wood vinegar was then subjected to physical and chemical tests as follows:

Color

The color of the wood vinegar extracted from two different coconut parts were determined by qualitative examination by 5 random respondents using their sense of sight. The perceived majority of color according to the respondents was recorded as the color of the wood vinegar.

Odor

The odor of the wood vinegar extracted from two different coconut parts were determined by qualitative examination by 5 random respondents using their olfactory sense. The perceived majority of odor according to the respondents was then recorded as the odor of the wood vinegar.

pH

The pH of the wood vinegars extracted was determined by using a pH paper. The tip of the pH paper dropped with 3 drops of vinegar samples and the paper was subjected to an indicator for numerical data and recorded. Testing was done in triplication.

Miscibility

Miscibility is the property of a liquid substance to mix in a given solvent. In this test, four (4) solvents namely; 96% ethyl alcohol, benzene, 10% H_2SO_4, and 10% NaOH was used as solvents to determine the solubility of the wood vinegars coming from different parts of the coconut tree. About 2 drops of sample was added to 1 mL of solvent and shaken. It was then allowed to stand for 10 minutes and the results were recorded. Three trials were done on each solvent.

3.6 Composition of Wood Vinegar

Composition of the wood vinegar which was extracted from coconut shells and coconut wood was determined using the procedures from Theapparat Y., Ponglimanont C. and Leelas-uphakul W. (2014).

Acid Content

The total acid content (TAC) and ionization characteristics was evaluated using titration with 0.1 N NaOH whose content was calculated from the volume of the titrated NaOH at pH 8.15 at the termination point of acetic acid, a major organic acid in the wood vinegar (Mun et al., 2007). The NaOH concentration was standardized with 0.1 N potassium hydrogen phthalate.

3.7 Soluble Tar Content

The total soluble tar content was evaluated by transferring a portion (0.5 g) of crude wood vinegar to a calibrated vial and heating at 105 °C overnight to remove any volatile components. The obtained residues were used for calculation of the tar content.

3.8 Water content determination

Titration was used to determine the amount of water in the wood vinegar samples. The titrator was calibrated with dry methanol. Then, 200 µL of wood vinegar was dropped in a container and titrated with the Karl Fischer reagent until reaching the end point. The results were the mean water content ± the relative standard deviation (measured as the percent milligrams of water per milliliter of sample) of three different measurements of each sample.

3.9 Basic and Neutral substances

Qualitative and Quantitative analyses were done using Gas Chromatography and Mass Spectrophotometry (GC/MS) to determine the present and enumerate the substances found in the crude wood vinegar extracted from coconut shell and coconut wood.

IV. RESULTS AND DISCUSSION

Acetic acid is, among other substances, produced by the dry distillation of wood (Phywe, 2017).

The following results were obtained after the testing of crude wood vinegar extracted using the procedures from Phywe (2017) in which the acetic acid (as primary acid) is formed. Also, methanol is formed just as the same time as acetic acid which is from the methoxy groups of the Iignins. The acetic acid content of the distillate is approximately 6%, which is about three times higher than that of methanol.

Also, it was observed that coconut shell when subjected to dry distillation gives more wood vinegar in terms of actual yield than coconut wood, all of which the two samples where thoroughly dried under sunlight for 6 hours.

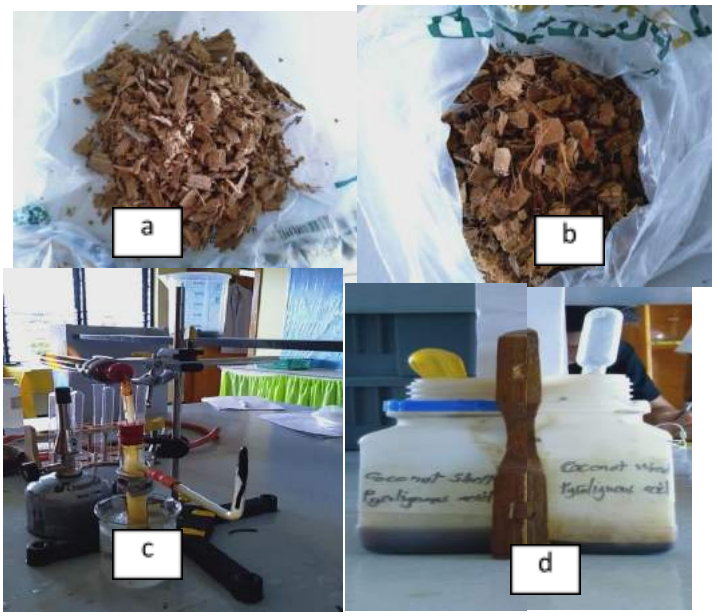

Figure 3: (a) coconut wood; (b) coconut shell; (c) dry distillation; (d) wood vinegars

Physical Properties

The physical property results are herein numerated:

Color and Odor

Table 1: Color and Odor of Wood Vinegars extracted from two (2) samples

	Physical Properties			
	CW Wood Vinegar		CS Wood Vinegar	
	Color	Odor	Color	Odor
R_1	Orange	Smells like burnt wood	Reddish orange	Burnt paper
R_2	Dark orange	Copra-like odor	Yellowish brown	Copra-like odor
R_3	Brown orange	Woody odor	Orange brown	Copra-like odor
R_4	Orange	Copra-like odor	Reddish orange	Copra-like odor
R_5	Dark orange	Copra-like odor	Yellowish brown	Copra-like odor

**CW – coconut wood; CS – coconut shell*

The majority of respondents indicated the color of the wood vinegar extracted from the coconut wood at a range of orange to dark or brown orange. Also, in terms of its odor, the wood vinegar from CW smells like copra, as described by most of the respondents.

Whereas, the wood vinegar from coconut shell was described by the respondents to be reddish brown to yellowish brown in color range, also, in terms of odor, the copra-like odor was the majority of description as stated by the respondents. This states that, certain chemicals that specify the distinctive color and smell of coconut wood vinegar are present.

Miscibility

In terms of the wood vinegars' miscibility, the following results were obtained:

Table 2: Miscibility of the extracted wood vinegar from the two (2) samples

	CW Wood Vinegar			CS Wood Vinegar		
	T1	T2	T3	T1	T2	T3
96% Ethanol	M	M	M	M	M	M
Benzene	IM	IM	IM	IM	IM	IM
10% H_2SO_4	M	M	M	M	M	M
10% NaOH	M	M	M	M	M	M

**M – miscible; IM – immiscible **CW – coconut wood; CS – coconut shell*

The table above show that the wood vinegar extracted from CW and CS are miscible to basic, acidic and alcoholic medium, but in contrast, the wood vinegar samples are immiscible to non-polar organic solvents. This indicates that one of the best methods for administering wood vinegar is the use of polar organic or inorganic solvents for various agricultural procedures.

pH

pH pertains to the acidity or alkalinity of the substance, the following table indicates that pH of the wood vinegar samples:

Table 3: pH of the extracted wood vinegar from the two (2) samples

	CW Wood Vinegar	CS Wood Vinegar
T_1	2.0±0.28868	2.5±0.28868
T_2	2.5±0.28868	2.0±0.28868
T_3	2.0±0.28868	2.0±0.28868
Average	**2.1667**	**2.1667**

**CW – coconut wood; CS – coconut shell*

Table 3 above show that the wood vinegar extracted from both coconut wood and coconut shell has a highly acidic pH. This acidity can be attributed to the presence of acetic acid and other pyroglinous acids that are products of destructive distillation of wood. This result is highly off the standard pH of wood vinegar which is between 2.5 to 3.0.

Acid Content

Acid content is the amount of acid that is present in the wood vinegar. It pertains to all acidic substances other than acetic acid which is one of the main chemical substances present in wood vinegar. According to Phywe (2017), acetic acid is approximately 6% of the total acid present in all wood vinegar samples. Acid content is herein shown below:

Table 4: Total Acid Content (TAC) of extracted wood vinegar from the two (2) samples

	CW Wood Vinegar (% by weight)	CS Wood Vinegar (% by weight)
T_1	6.47±0.21385	6.98±0.18520
T_2	6.61±0.21385	6.63±0.18520
T_3	6.89±0.21385	6.91±0.18520
Average	**6.6567**	**6.8400**

Average wood vinegar TAC was between 6.65 and 6.84 percent by weight as calculated at pH 8.15 using 0.1 N Sodium Hydroxide as titrant. This indicates that acid content of both wood vinegars from coconut wood and shell are slightly higher than the expected TAC present in most wood vinegars which is 6% by weight.

4.1 Soluble Tar Content

Soluble tar is the number of organic tar dissolved in the wood vinegar matrix. Soluble tar is herein tabulated in the subsequent table:

Table 5: Total Soluble Tar (TST) of extracted wood vinegar from the two (2) samples

	CW Wood Vinegar (% by weight)	**CS Wood Vinegar** (% by weight)
T_1	0.28±0.01528	0.31±0.01155
T_2	0.30±0.01528	0.33±0.01155
T_3	0.27±0.01528	0.31±0.01155
Average	**0.2833**	**0.3167**

Total Soluble Tar (TST) is the amount of soluble tar that is dissolved in the wood vinegar. It can be observed that the two samples of wood vinegars contain small amounts of soluble tar which is an indication of the degree of purity of the extracted wood vinegar. Also, this result coincides with the Japanese standard that dissolved tar content should not be more than 3% (Wada, 1997).

4.2 Water Content

Water content is the amount of moisture or water molecules present in the wood vinegar samples. The water content of wood vinegar samples from coconut wood and coconut shell are herein tabulated:

Table 6: Water Content of extracted wood vinegar from the two (2) samples

	CW Wood Vinegar (% by weight)	CS Wood Vinegar (% by weight)
T_1	80.2±0.45826	90.3±0.20000
T_2	80.8±0.45826	89.9±0.20000
T_3	81.1±0.45826	90.1±0.20000
Average	**80.7**	**90.1**

It was observed that the coconut shell has higher water content than coconut wood. This result is higher than two commercially produced wood vinegar which possesses less water content at a range of 80.49 and 79.18%, respectively (Theapparat, Yongyuth & Chandumpai, Ausa & Leelasuphakul, Wichitra & Laemsak, Nikhom & Ponglimanont, Chanita., 2014).

4.3 Basic and Neutral substances

Other substances were also found present in the wood vinegar. Here are the some of the many chemical compounds found in the two (2) samples:

Table 7: Other Substances found in Wood Vinegar Samples

	Chemical Compounds	% Concentration on CW WV	% Concentration on CS WV
1	Alkyl aryl ether	34.045	32.665
2	Phenol	30.224	28.799
3	Nitro-2-methyl-2-butane	10.006	11.120
4	2-methyl propyl ester butanoic acid	7.988	9.098
5	2-methoxyphenol	6.879	5.006
6	2,6-dimethoxyphenol	6.541	7.074

Percent concentration is the total concentration of other substances in the remaining 4-5 % of the unknown compounds present in the wood vinegar samples. Other trace chemicals are also found such as 9-octadecenoic acid (Z)-tetradecyl ester-(Oleic acid, tetradecyl ester)-$C_{32}H_{62}O_2$, 2-lauro-1,3-docecoin-$C_{35}H_{66}O_6$, dedecanoid acid, 1,2,3-propanetriyl ester (glyceryl tridodecanoate) -$C_{39}H_{74}O_6$, octanoic acid, Syringol, 1-(4-hydroxy-3,5-dimethoxyphenyl)-ethanol and 1-(4-hydrox y)-4-hydroxytoluene. These chemicals can be further utilized for agriculture, aquaculture, soil fertilizer, antimicrobial, antioxidant, flavoring, latex coagulant, sheet additive, wood preservative, pesticide, plant growth enhancer, antifungal, feedstuff and even repellent or insecticide.

V. CONCLUSIONS

Based on the results of the study, the following conclusions are herein drawn:

1. Clear to dark orange is the color of wood vinegar extracted from coconut wood, while yellowish to dark yellow orange was observes on wood vinegar from coconut shell, both have a copra-like odor as perceived by most of the respondents.
2. High pH was observed on both wood vinegar samples and its miscibility was observed to be high on most polar solvents, but is immiscible to non-polar solvents.
3. Slightly high TAC was recorded on both the wood vinegar samples which are slightly higher than the allowable percentage for wood vinegar which is 6%.
4. In terms of soluble tar, a very low percentage was observed on both the samples which are <1% which coincides with the Japanese standard that dissolved tar content should not be more than 3%.
5. For water content, wood vinegar from coconut shell has a higher percentage presence than wood vinegar from coconut wood at 80.7 and 90.1 percent, respectively indicating a high percent of moisture presence in the extracted wood vinegar samples.
6. In terms of basic and neutral substances, Alkyl aryl ether, Phenol, Nitro-2-methyl- 2-butane, 2-methyl propyl ester butanoic acid, 2-methoxyphenol, 2,6-dimethoxyphenol were the most common substances found in the two samples with varying percentage composition, also other trace chemicals were observed using GC-MS analysis.

REFERENCES

1. Bess R, 2016. How to Test the Specific Gravity of Liquids. Retrieved at: https://ww

w.wikihow.com/Test-the-Specific-Gravity-of-Liquids.
2. ECHO, 2012. An Introduction to Wood Vinegar. Technical Note 77.
3. Food and Fertilizer Technology Center 2010. Wood Vinegar. Retrieved at: http://www.fftc.agnet.org/library.php?func=view&id=20110720153306.
4. Office of Her Royal Highness,, (n.d.). Benefits of Wood Vinegar. Princess Maha Chakri, Sirindhorn's Projects, Thailand.
5. Payamara, J. Usage of Wood Vinegar as New Organic Substance. International Journal of ChemTech Research. Vol. 3 (3), pp1658-1662, 2011.
6. Phywe 2017. The Characterization of Acetic acid "Wood Vinegar". Teacher's/ Lecturer's Sheet. Tess Advanced.
7. Theapparat, Yongyuth & Chandumpai, Ausa & Leelasuphakul, Wichitra & Laemsak, Nikhom & Ponglimanont, Chanita. (2014). Physicochemical Characteristics of Wood Vinegars from Carbonization of Leucaena leucocephala, Azadirachta indica, Eucalyptus camaldulensis, Hevea brasiliensis and Dendrocalamus asper. Kasetsart Journal - Natural Science. 48. 916-928.
8. Wada, T. 1997. Charcoal Handbook. Forest management section, agriculture, forestry and fisheries division, Bureau of labour and economic affairs, Tokyo Metropolitan Government. Tokyo, Japan: 92 pp.
9. Yokomori, M., 2011. Farmers in Benguet Practice Savers Technology. Safe Vegetable Promotion Project in Benguet.

Towards an Urban Solution – Semi Automated Car Parking in Doha, Qatar

Arch. Ahmed R. Hammad

ABSTRACT

In light of the increasing number of vehicles in urban and semi-urban cities, the need to provide adequate car parking is becoming more essential to accommodate the increased number of vehicles (1). Due to the increasing price in land, providing a traditional car parking solution is not practical nor feasible. Therefore, designers had to articulate different behaviors and more efficient solutions to this issue.

On the other hand, providing adequate car parking is always a major obstacle in any project; thus, in most cases, the outcome of the design is insufficient car parking spots to the bare minimum of the requirement. In most countries, the legislation or design code for commercial or residential buildings provides minimum car parking spaces with minimum spaces for visitors or deliveries, and if provided, usually the parking spaces are insufficient, and this is comprehensible due to the high cost of land and construction.

Keywords: semi-automated car park, adequate car parking, commercial building in Doha – Qatar.

Classification: FOR Code: 091302

Language: English

London Journals Press

LJP Copyright ID: 392986
Print ISSN: 2631-8474
Online ISSN: 2631-8482

London Journal of Engineering Research

Volume 21 | Issue 3 | Compilation 1.0

Towards an Urban Solution – Semi Automated Car Parking in Doha, Qatar

Arch. Ahmed R. Hammad

ABSTRACT

In light of the increasing number of vehicles in urban and semi-urban cities, the need to provide adequate car parking is becoming more essential to accommodate the increased number of vehicles (1). Due to the increasing price in land, providing a traditional car parking solution is not practical nor feasible. Therefore, designers had to articulate different behaviors and more efficient solutions to this issue.

On the other hand, providing adequate car parking is always a major obstacle in any project; thus, in most cases, the outcome of the design is insufficient car parking spots to the bare minimum of the requirement. In most countries, the legislation or design code for commercial or residential buildings provides minimum car parking spaces with minimum spaces for visitors or deliveries, and if provided, usually the parking spaces are insufficient, and this is comprehensible due to the high cost of land and construction.

However, some elite developers market the extra car park as their selling point for their developments or even offer the additional car park for sale when required. Nevertheless, this does not resolve the problem of the inadequate car park; on the contrary, it complicates the matter.

This paper will discuss the solution provided for a commercial building in Qatar – Doha while providing a semi-automated car parking system to resolve the insufficient number of car parking provided. The commercial building is located in old Doha downtown where the building was constructed more than 20 years ago, and the legislation by then were less stringent. The initial solution provided by the developer was to use the neighboring land as a car park for the tenants. Thus, this was still insufficient.

For most tenants, having allocated car parking is a must to have in addition of providing visitors car park. This will make the commercial spaces attractive for tenants and users, especially when there isn't public transportation connected with the development?

Keywords: semi-automated car park, adequate car parking, commercial building in Doha – Qatar.

Originality/value

This paper will present a solution proposed and executed by a private developer for a commercial building located in the old city of Doha downtown to resolve the insufficiency number in car parking spots. The paper will discuss and explain the design and the technical solution realized at site which has successfully resolved the car parking issue.

I. INTRODUCTION

Doha is the capital city of Qatar and the political and economic center yet the most populous city with a population of 956,460 (2015) (2). The city is located on the coast of the Persian Gulf and it is the fastest-growing city. Qatar has seen a huge growth in population in the past decade (3) which is directly connected to the economical and real estate boom which has affected the gulf area. The population growth has been attended by a significant increase in the number of vehicles which has led to parking problems (3).

The design guidelines introduced by the authorities have regulated the number of car parking provided for each development and use. The purpose of these guidelines and regulations is to ensure that sufficient car parking is provided

London Journal of Engineering Research

by the objective of the zoning and regulations of each area (4). Tale (1) below reflects the required onsite car parking rate as set by the regulatory authority. As per the guidelines stipulated in the table, the design will provide 1 car parking for each 1- or 2-bedrooms unit if the area is less than 120 sqm.

Table 1: Required parking rate

USE	RATE	CAR PARK RATE/NOTES
Residential Unit/Dwelling		
All residential Units and Dwellings	1	For each one- or two-bedroom dwelling or each 120 Sqm GFA plus 0.25 car parking spaces per dwelling for visitors
	2	For each three or more-bedroom dwelling plus 0.25 car parking spaces per dwelling for visitors
Worker Accommodation	N/A	Subject to Traffic Impact Assessment

The above reference is feasible for developers and owners since the land price is too high to accommodate more car parking. Nonetheless, such guideline is not practical nor realistic as a family with two working independents will acquire two cars. The same applies to commercial buildings as the code requires one car park for every 65 sqm (4). In an average office space of 500 sqm, the provided car parking will be approx. 8. The average space per employee in an office is around 12-14 sqm per person (5). Based on this, the average number of employees will be 38 employees. If we assume that 50% of the employees own a car, this means that the required car parking will be 19 car parking excluding visitors, whereas the provided number of parking spaces is eight.

As mentioned earlier, the standard codes are based on the overall urban study of the area and zoning, taking into account public car parking, public transportation, and other wider considerations. Nevertheless, the inadequacy of car parking is always a problem in most areas.

II. METHODOLOGY

The selected car parking area was identified as a prototype location to design and implement the semi-automated car parking system. The plan was redesigned to accommodate the semi- automated parking dimensions, then the order was sent to the manufacturer. While the system is being manufactured, some ground preparation works have to be prepared.

Dismantling of existing structures (if any). In the case of the subject project, there were existing car parking sheds which needed to be dismantled.

Following that, the ground was asphalted. However, the manufacturer's recommendations called for a concrete base of 10x15 cm to be casted at each corner of the system. The concrete block should be cast at a certain level in accordance with manufacturer recommendations. The electrical circuit should be arranged with a single point connected to each car park unit. The above work should be ready and organized prior to receiving the system. Once the machines are shipped to the site, a specialized installation team will carry out the system installation and carry out the required testing and commissioning of the system. Once the work is completed, a comprehensive training and troubleshooting session will be carried out to the operation team.

2.1 FIFA 2022 World Cup in Qatar

The state of Qatar has spared no effort and extensive preparations to earn and host such an

international event, which is the first time being held in the middle east and North Africa region (6). For such event, a wide-ranging study have taken place for each stadium to validate the success of the operational aspect. With such an event taking place, the impact on other cities and sub-cities will be significant even if those areas are not involved directly with this great event. In other words, many professionals have moved and lived in the city of Doha, occupying additional residential and commercial spaces working on other subdivisions related to the world cup project. This increase of workers, professionals, and their families has certainly impacted the availability of sufficient car parking in these areas.

This paper will not discuss the impact of such an important event on the urban fabric of the city, however, as highlighted in the introduction of this paper, the parking matter already exists, and such event will impact the overall city. Though the authorities are working on solutions on a large scale to overcome this issue, private developers and owners entail resolving their particular parking issue by themselves. This paper will

discuss the solution proposed and executed by a private developer to overcome their specific shortage in car parking to stand out from other competitors.

2.2 The system

The automated car parking system is a mechanical system which is designed to reduce the area utilized by cars (7). The automated car parking system provides car parking on multi-vertical levels to increase the number of parking spots while reducing the plot required for the same number of cars.

The original concept for this invention was founded in Paris in 1905 (8). The idea was based on the car's elevator concept built in a multi-story concrete building.

The saved space provided by this system results from reducing the associated spaces with the car parking itself. These associated spaces are (9):

- The distance between cars is eliminated as no space is required for cars to park in, maneuver, or open doors.
- No ramps are required to drive cars in or out
- Ceiling heights can be reduced to the minimum
- Walkways, elevators, and staircases will not be required.

There are other simpler systems where the idea is to duplicate the number of car parking by simply adding another car park at the top of the existing one. By applying this idea, the total number of cars is simply duplicated.

Below figure (1) illustrates the different types of automated car parking systems

Figure 1

III. MECHANICAL PARKING

In this paper, the discussion will focus on one type of automated car parking system which is mechanical parking as this solution was realized in the subject project. This solution is usually applied when the car parking is already executed, and the requirement is to double the number of car parking. Also, it requires less disruption to the area with the least construction and excavation works. Below figures (2) and (3) illustrate the different positions of mechanical car parking and how the solution doubles the capacity of car parking.

Figure 2

Figure 3

Below figure (4) is a detailed drawing reflecting the automated car parking system. The installation procedure is straightforward and modest as it does not require any excavations or lift pit, just a concrete base under each corner that can cast on top of the existing surface.

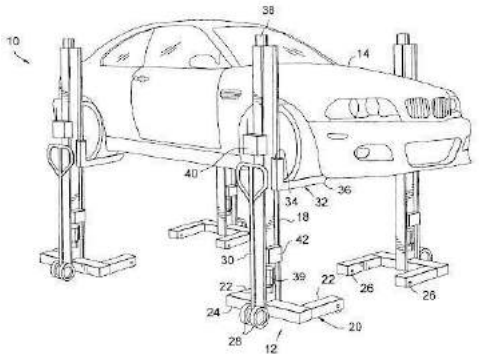

Figure 4

3.1 The Location

The project subject is located in the old city of Doha at the interchange of the so-called Banks Street. The area is considered the city center of the old city of Doha and a great tourist attraction (10).

Main tourists' attractions next to the project are:

- Souq Waqif: or the standing market. An old open market was renovated in 2006 that sells traditional handicrafts, garments, and other souvenirs along with multiple restaurants. The original building goes back to the 20th century as recorded (11). During the renovation, a large car parking area was created under the complete Souq as two basements to accommodate for the great number of cars. As per the official site of the Souq, the car parking can easily place 2400 cars with a subsidized rate per hour to encourage visitors and tourists to visit this destination. The parking solution has helped the area dramatically as it reduced the pressure on all surrounding shops, retails and office buildings. Many users and visitors utilize this parking if they are in the area.

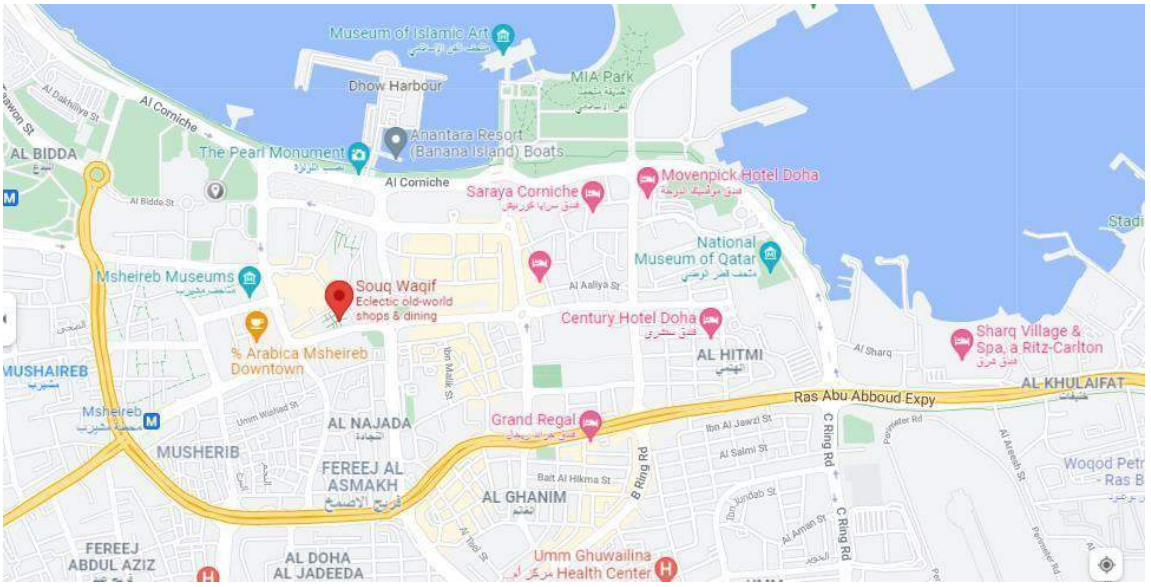

Figure 5

Figure 6

Figure (5) above shows the location map of the Souq, and figure (6) reflects the overall configuration of the project

Musheireb City: a commercial district that will revive the old Souq idea with a new architectural language. The project will consist of around 100 buildings of offices and retails and will have approx. 10,000+ car parking (12). The target of this project is to become the new social and civil hub in the city center, a place to work, live, visit and shop. The project has provided sufficient car parking in the overall development as the surrounding area is congested and it is intolerable to find a car park in the district as reflected in below figures (7) and (8).

Figure 7

London Journal of Engineering Research

Figure 8

From both locations described above, it is noticed that the area is congested with many tourists attractions where car parking is a major issue. Also, many other office buildings and major banks are located in the same area where employees endure finding car parking every day. The same applies to the project case study as it is an office building located in the same area.

IV. CASE STUDY

4.1 Project Description

The building is called Alfardan Center, one of the venerable iconic buildings in that area (13), built around two decades ago in this prime location. A commercial building with one basement level and retail at the ground floor (street level), then seven levels of office spaces (14). The building is within a few steps from Souq Waqif and very close proximity to Musheireb city.

Figure (9) below reflects the exterior image of Alfardan center building and figure (10) a reference floor plan.

Figure 9

Figure 10

Figure 11

Figure (11) above is the location map for the project subject which clearly shows the proximity to other vital focal points explained in this paper earlier.

The estimated usable space per floor is 500 sqm, and as per the authority's parking code for office spaces mentioned above, the required car parking will be eight cars per floor. Hypothetically, if it is assumed that the eight floors are used as office spaces, this means that the total usable area will be 4000 sqm. Consequently, the required car parking will equate to 64. The building design has provided the authority required number of car parking, assuming that an adequate number of employees and visitors will use the public transportation since the building is adjacent to a bus and metro station. Nevertheless, and since the cost of acquiring a car in Qatar is reasonable for most workers, the majority owns a car and tend not to use public transportation. Thus, more car parking spots will be required to accommodate this increase in cars. Based on the Australian standards for offices spaces referred in this paper, the 4000 sqm of office space will accommodate roughly 250-300 employees, and assuming that 50% of them owns a car, then the required car parking will be 125-150 car parking which is not feasible nor logical to be provided in any commercial building as this will be additional construction cost and will have a major impact on the roads system traffic.

To accommodate the required parking spaces for the eight floors, employees and visitors occupy the basement parking along with the other two areas marked in orange in the below figure (12).

Figure 12

The plot adjacent to the project is part of the building property and used as an employee's parking (Figure 13 below). The capacity of this parking is 37 covered car parking.

Figure 13

The automated car parking project was executed in this parking where the parking spots have increased from 37 to 61 car parking. The solution was to remove all existing covered car parking and to install the automated system which allowed double parking in each spot. The below Figure 14 shows the revised layout plan accommodating all 61 cars in the area, which used to accommodate 37 cars only. Due to the site constraints, the system was installed to receive 58 cars in double- stacked, and 3 cars were kept as a conventional parallel parking. As noticed from the drawing, the entry and exit of the parking remained as the original parking.

Figure 14

The solution was particle and cost-efficient as no major infrastructure works were involved. A flat concrete bedding was cast on the complete area then the specialized company installed the machines directly on the concrete base.

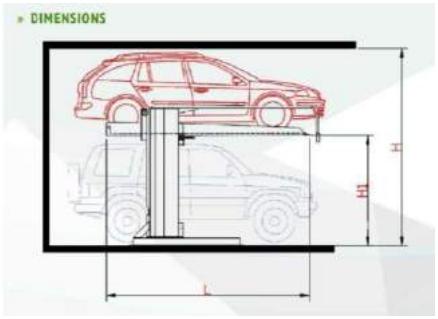

Explanation		Majorlift
Height Clearence	H	320-350-400 cm
Clearence Each Deck	H1	150-215 cm
Platform Lenght	L	370 cm
Inner Width	W1	190-230 cm
Total Width	W	226-266 cm
Lifting Capacity		3000 kg
Lifting Speed		45 sn.
Motor		2,6 kw / 3 Phase
Total Weight (Unloaded)		1260 kg

Figure 15

Figure 15 above, shows the required dimensions for such a system in plan and section. Also, the system can be installed directly on a flat surface with no need for any deep excavations.

The system was connected to the existing power supply as the power usage is minimal. The only disadvantage of this system is the operations, as it requires a full-time standby operator to organize the cars maneuvering and lift them. Nevertheless, this solution has provided almost double the capacity without executing a complicated structure or to build a basement structure with ramps.

Figures (16), (17), and (18) below show the mockup which was executed at the site as a mockup in order to take the exact measurements prior to the final production.

Figure 16

Figure 17

Figure 18

V. CONCLUSION

In most the cities and especially downtown, conventional parking has reached its limits in most developments. The increasing number of vehicles in cities and sub-cities, and with the limited capabilities of conventional car parking, has created lots of parking jams, double and illegal parking, which all led to roadblocks. A convenient and fastest way to resolve such an issue is to apply a semi-automated car parking solution. This solution utilizes the existing parking area, and through installing semi-automated machine, the space is doubled. Recently there have been several projects utilizing such a system. However, it hasn't reached a level where authorities and owners believe that such system will help to resolve the problem.

Application

This parking system is applicable where parking spaces and budgets are limited. Such a solution can be implemented immediately and can be applied in low to moderate capacity commercial

buildings, car showrooms where cars can be stored for a longer period. The downside of such a system is the operation. A full-time operator such as – car valet – has to be present at the site during the operation hours to manage and operate the system.

Also they will be responsible parking the cars in and out. In busy commercial sites where cars are required to be parked in and out in a faster mood, other fully automated systems can be used. In some long-term parking such as airports, or where employees spend long hours at their offices, such system can be applied.

ACKNOWLEDGMENT

This paper is fully supported by: Prof. Dr. Arch. Rizeq N. S. Hammad, Jordan University, Amman, Jordan. His continuous support, reviews and, inspiration are countless.

REFERENCES

1. Sk. Md. Golam Mostafa, Multilevel Automated Car Parking System.
2. VisitQatar.com
3. Pande, Anurag, Classification tree analysis of factors affecting parking choices in Qatar.
4. Qatar National Master plan, Additional guidance, Car parking regulations.
5. The Building code in Australia.
6. Traffic Impact Assessment for the Stadiums Hosting FIFA 2022 World Cup in Qatar: A Case Study.
7. Patrascu, Daniel (2010), "How Automated Parking Systems Work.
8. Sanders McDonald, Shannon."Cars, Parking and Sustainability.
9. Staff, Greenandsave (2012), "Automated Parking And Garage Lights Take "Green" Garages To New Levels".
10. Qatar Ministry of Municipality and Urban Planning.
11. Souq Waqif Doha.
12. www.msheireb.com/msheireb-downtown-doha/about-msheireb-downtown-doha/
13. www.alfardanproperties.com/property/alfardan-centre/
14. http://www.cdc-qatar.com/CDC/Al-Fardan-Centre.